ON THE ESTIMATION OF POROSITY IN COMPOSITES BY OBLIQUE ANGLE ILLUMINATION

A.C. Kak, Mani Azimi and Malcolm Slaney

School of Electrical Engineering
Purdue University
West Lafayette, IN 47907

ABSTRACT

Reported here are some preliminary computer simulation results on the feasibility of using oblique incidence ultrasound for the detection and estimation of porosity in composites. In the oblique incidence approach, the composite is illuminated at off normal angles in such a manner that the reflected returns from the fibers are in directions away from the illuminating transducer. Since the scattered returns from porosity tend to be more omnidirectional than the fiber returns, there is a larger received signal in the presence of porosity.

INTRODUCTION

To illustrate where the porosity occurs in a composite, we have shown in Fig. 1 a hypothetical two-ply graphite-epoxy composite. Each ply is approximately 100 microns thick, consisting of fiber laminae stacked on top of each other. The fiber diameter is about 10 microns and there are approximately 10 laminae in each ply. Most of the porosity is concentrated between the plies, although some of it does permeate into the plies themselves. In most cases the porosity may be modeled as consisting of spherical voids of about the same diameter as the cylindrical fibers. Because of its bearing on the mechanical properties of a composite, it has become important to be able to develop nondestructive procedures for its detection and for the estimation of its distribution.

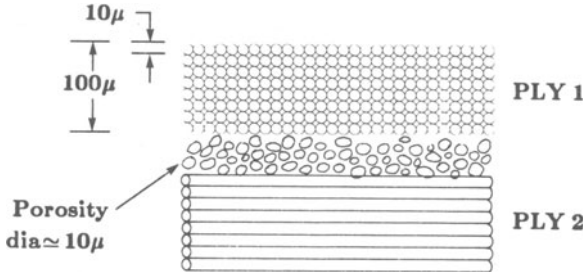

Fig. 1. Depiction of porosity in a graphite-epoxy composite.

CAN THE SPECTRAL DISTRIBUTION OF ECHOS BE USED FOR THE ESTIMATION OF POROSITY PARAMETERS?

It was clear from the beginning that the spectral analysis of backscattered data would not be of much use for either the detection of the porosity, or the estimation of any of its parameters. To illustrate the futility of developing any techniques based on such an approach, consider the frequency domain periodicities induced by the returned echos by each void. Shown in Fig. 2a is a 10 micron void illuminated with a broadband pulse. The returned signal will consist primarily of two echoes, one corresponding roughly to the front tangential plane AA', and the other corresponding to the creeping wave with a delay approximately equal to $\pi a/v$. With an experimentally determined bulk propagation velocity, v, of 4500 m/s, this translates into a delay of around 4 ns between the two pulses. As illustrated in Fig. 2b, the corresponding frequency domain periodicity for this delay between the pulses is equal to 250 MHz, which is totally outside the bandwidth of the experiments we have in mind. It is equally easy to show that with broadside illumination the periodicities in the frequency domain by the 180° backscatter from different voids will also be outside a reasonable (low MHz) bandwidth.

It can also be shown easily that even if we use the arrangement shown in Fig. 3 where the transducer is located in a directional window where because of the directional properties from the fibers, not much fiber return is expected, the spectral periodicities will in most cases be too large to be of much use in low MHz experiments. Even if the spectral periodicities were conveniently located in the measurement bandwidth, we will now show with a simple analysis that they will be obliterated by the periodicities introduced by the geometry of the illumination. In order to illustrate this point, first note that if d is the mean distance between voids, this distance being measured in planes parallel to the plies, and if the reception angle is very oblique, as shown in Fig. 3a, the frequency domain periodicity corresponding to this distance would be $1/\tau_d$, where τ_d is approximately equal to $2d/v$. For v equal to 4500 m/s,

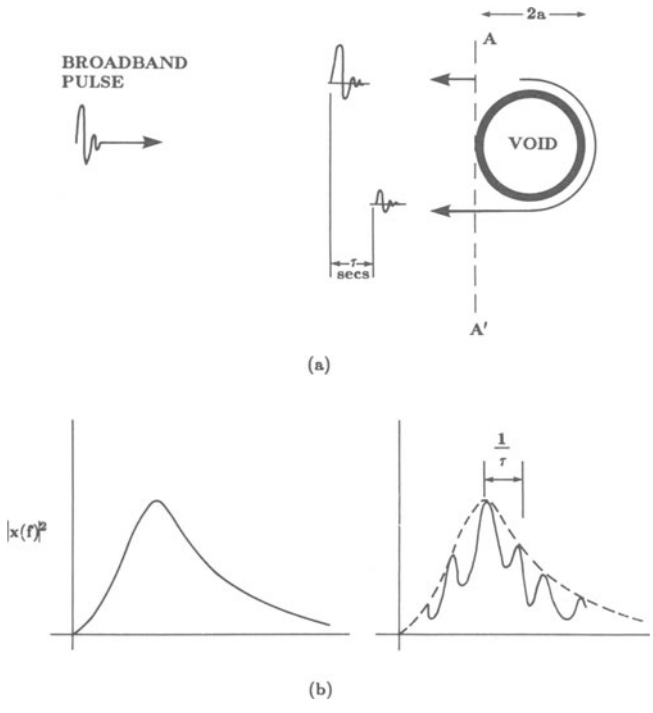

Fig. 2. (a) When a broadband pulse illuminates a void, the backscattered return is roughly a superposition of an echo corresponding to the front tangential plane AA' and a creeping wave backscatter as shown. (b) $|X(f)|^2$ represents the power spectrum of the broadband illumination in (2). Shown on the right are the periodicities in the received power spectrum corresponding to the two echos in (a).

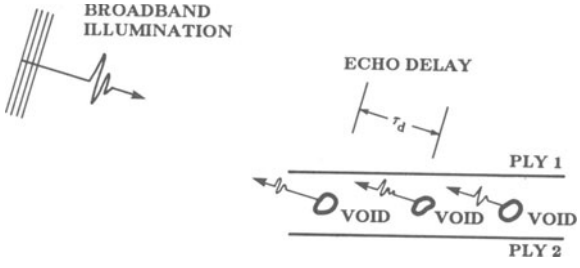

Fig. 3. Shown here is broadband illumination incident on the porosity at a very oblique angle.

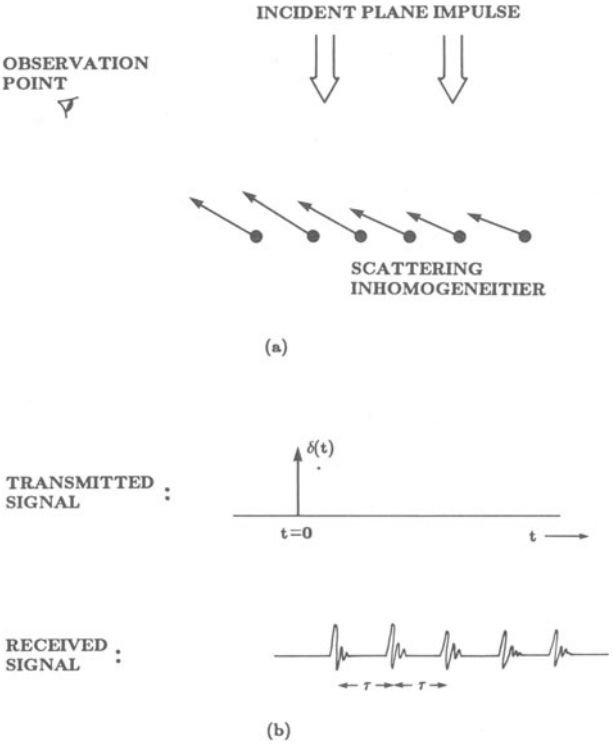

Fig. 4. (a) Shown here are a finite number of inhomogeneities being illuminated by a plane wave impulse. (b) The illumination impulse and the received signal are depicted here.

this frequency domain periodicity is between 2.5 MHz and 25 MHz for d ranging between 100 microns and 1000 microns. To show how these periodicities are distorted by the geometry of illumination, we will consider a grossly simple model of scatter from a series of inhomogeneities that are approximately uniformly spaced within the beamwidth of the illumination, as shown in Fig. 4a. (We are using this utterly simplistic model only to bring out the frequency domain distortion caused by the illumination parameters.) Assuming that the illumination is a plane wave in space and an impulse in time at the observation point shown in Fig. 4, the received signal is proportional to

$$\text{recd. signal} = \sum_{n=0}^{N-1} s(t-n\tau) \qquad (1)$$

where $s(t)$ is the impulse response of the scattering process from each inhomogeneity and τ is the delay between the successive arrivals at the observation point. To incorporate the actual time dependence of a broadband illumination, we rewrite the above equation as

$$\text{recd. signal} = y(t) * \left[\sum_{n=0}^{N-1} \delta(t-n\tau) \right] \tag{2}$$

where y(t) is a convolution of the function s(t) and the time dependence of the broadband illumination. In writing the above as the received signal we have ignored the transfer function of the receiving transducer. To investigate the periodicities of this function, we rewrite it as

$$\text{recd. signal} = y(t) * \left[\Pi\left(\frac{t}{T}\right) \times \sum_{n=-\infty}^{\infty} \delta(t-n\tau) \right] \tag{3}$$

where Π is a rect function with its base of support equal to T. For acute angles of reception, T is essentially the time of propagation across the illumination beam. Since, as shown below, the Fourier transform of a train of impulses in time domain is a train of impulses in the frequency domain:

$$F\left\{ \sum_{n=-\infty}^{\infty} \delta(t-n\tau) \right\} = \frac{1}{\tau} \sum_{n=-\infty}^{\infty} \delta\left(f-\frac{n}{\tau}\right) \tag{4}$$

and, since the Fourier transform of a rect function is a sinc function:

$$F\left\{ \Pi\left(\frac{t}{T}\right) \right\} = T \frac{\sin \pi fT}{\pi fT} \tag{5}$$

we may write the following expression for the Fourier transform of the right-hand side in Eq. (3):

$$F[\text{recd. signal}] = y(f) \left[\frac{T}{\tau} \sum_{n=-\infty}^{\infty} \frac{\sin \pi\left(f-\frac{n}{\tau}\right)T}{\pi\left(f-\frac{n}{\tau}\right)T} \right] \tag{6}$$

The frequency domain product on the right-hand side above is depicted in Fig. 5. It is clear that there will be two different periodicities in the output spectra, one corresponding to the distance between the inhomogeneities and the other corresponding to the width of the illumination beam. For a 100 micron distance between the spherical inhomogeneities, and a propagation velocity of 4500 m/s, the $1/\tau$ period between peaks of the spectrum is equal to about 50 MHz, again outside the range of frequencies used in low MHz experiments. The 1/T period is equal to about 3 MHz for a 3 cm wide illumination. Therefore in low MHz experimentation, the spectral periodicities will be completely dominated by the width of the illumination beam.

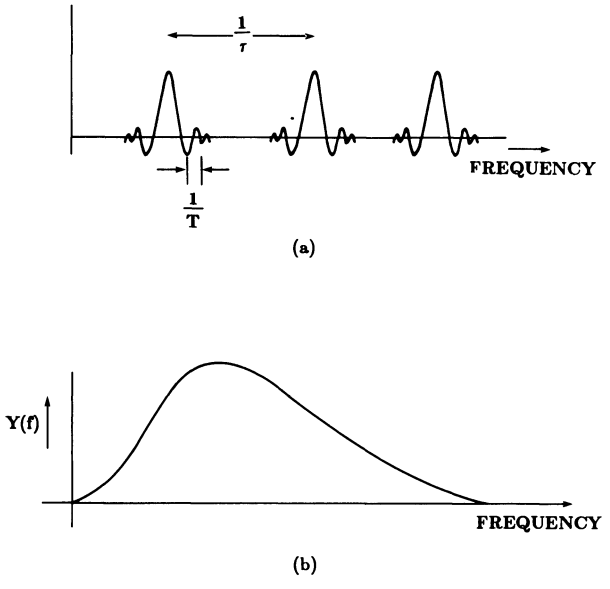

Fig. 5. (a) Shown here is the term in the brackets in Eq. (6). We see two types of periodicities: those with period equal to $1/\tau$, and those with period $1/T$. (b) The Fourier transform of the received signal is obtained by multiplying (a) with Y(f) shown here.

The above conclusion that for small diameter inhomogeneities tightly packed together, any periodicities in the received signal spectrum will be those corresponding to the illumination beamwidth is borne out by the following computer simulation results. Clusters of inhomogeneities packed in the form of rectangular strips, as shown in Fig. 6, were illuminated by a plane wave in computer simulation experiments. The cylindrical inhomogeneities were assumed to be weakly backscattering rigid fibers. The acoustic scattering from each fiber was calculated by using the following formula for pressure amplitude:[1]

$$P_s = \sqrt{\frac{2\rho ca}{\pi}} \quad \psi_s(\phi) e^{+jkr} \tag{7}$$

where ρ and c are, respectively, the density and the propagation velocity of the background medium. The radius of the fiber is represented by a and the scattering function $\psi_s(\phi)$ is given by

$$\psi_s(\phi) = \frac{1}{\sqrt{ka}} \sum_{m=0}^{\infty} \varepsilon_m \sin\gamma_m \, e^{-j\gamma_m} \cos m\phi \tag{8}$$

with $\varepsilon_0=1$ and $\varepsilon_m=2$ for $m > 0$. In (7) and (8) the wavenumber is denoted by k. The angles γ_m are given by

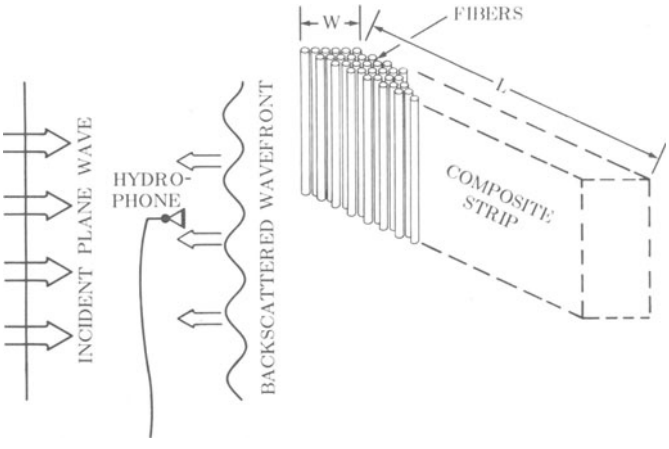

Fig. 6. Shown here is the backscattering problem that was computer simulated for investigations into the frequency domain periodicities of the returned echoes.

$$\tan \gamma_o = -\frac{J_1(ka)}{N_1(ka)}$$

$$\tan \gamma_m = \frac{J_{m-1}(ka)-J_{m+1}(ka)}{N_{m+1}(ka)-N_{m-1}(ka)} \qquad (9)$$

where J_m and N_m represent, respectively, the Bessel and the Neumann functions. In Fig. 7 we have shown the received scattered field for a 6 cm wide and 2.1 mm thick strip containing 500 fibers in each of the 15 layers. The radius of each fiber is 50 microns and the distance between the fibers is 120 microns. Compare the periodicities of this spectrum with that shown in Fig. 8 for the case of a strip of similar dimensions that, however, contains fibers of radius only 10 microns. In Fig. 8 we have again used 15 layers in the strip; however, each layer now contains 2500 fibers. The spectral periodicities in Fig. 8 are identifical to those of Fig. 7. One can only deduce that these are related to the overall geometry of the sample or the width of the illumination, both inducing identical effects. We have shown in Fig. 9 what happens to the spectral distribution when we slightly randomize the fiber locations in Fig. 7. In Fig. 9 the distance between the fibers is uniformly distributed between 100 microns and 140 microns.

DETECTION AND ESTIMATION OF POROSITY VIA ENHANCED SIGNAL RECEPTION AT OBLIQUE DIRECTIONS

After abandoning looking for porosity parameters in the spectral composition of the received signals, we turned our attention to the received power levels as a function of oblique angles for reception and perhaps also for transmission.[2]

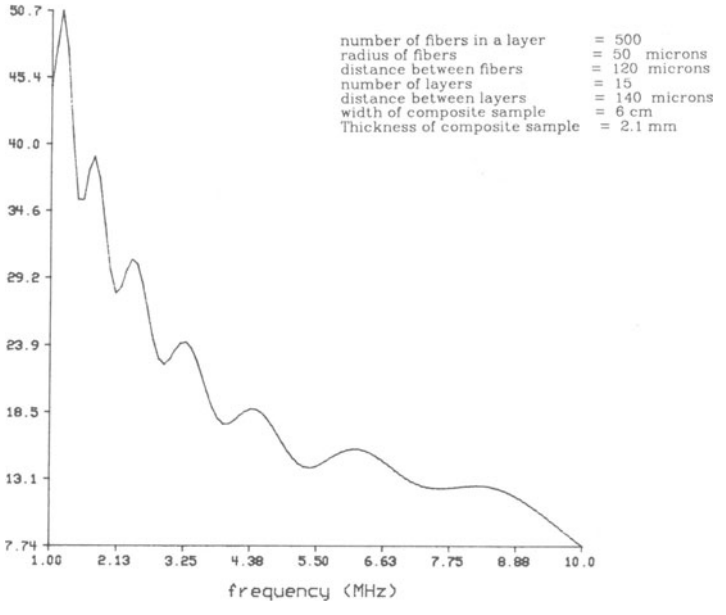

Fig. 7. Spectral composition of the returned signal for the parameters shown in the figure.

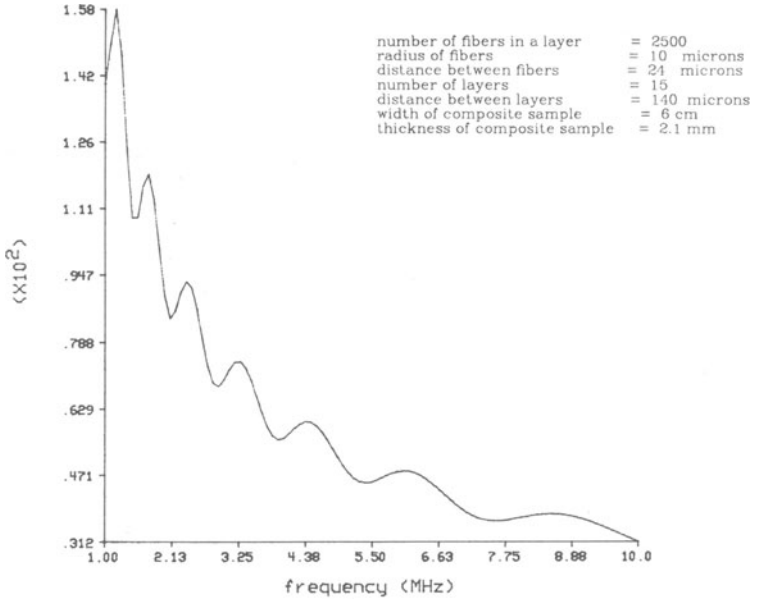

Fig. 8. Spectral composition of the returned signal for the parameters shown in the figure. Although the fiber density here is totally different from that in Fig. 7, the periodicities remain the same.

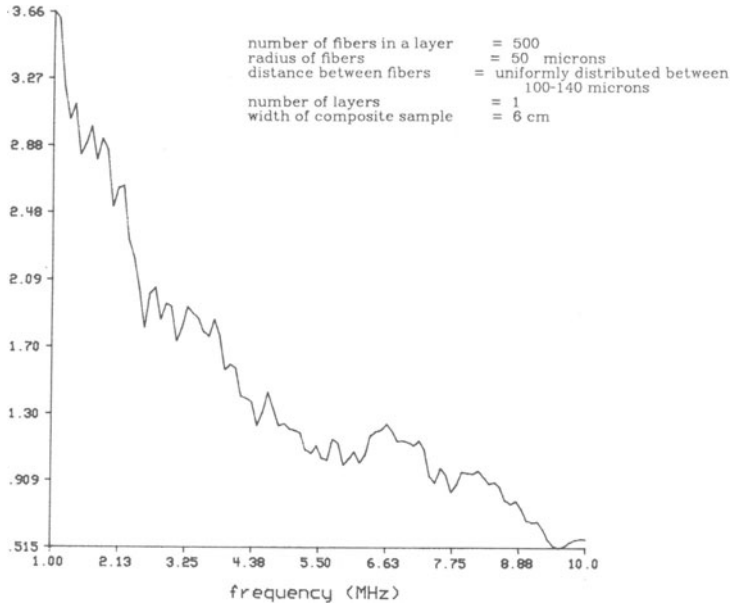

Fig. 9. Effect of randomization of fiber locations on the spectral composition of the returned signal.

We have studied by computer simulation the radiation problem shown in Fig. 10, where an ultrasonic transducer illuminates a ribbon of fibers over a cluster of voids. The purpose of the computer simulation was to bring out directional windows in which the scatter from the voids would exceed by measurable levels the scatter from the fibers.

In our computer simulations, the radiation from the transducer shown in Fig. 10 was expressed as a spectrum of plane waves as follows. Let (ξ,ζ) represent the coordinates in the plane of the transducer. In the (ξ,ζ,η) coordinate system, where the axis η is perpendicular to the (ξ,ζ) plane, the radiated field at any point, $\vec{r} = (\xi,\zeta,\eta)$, may be expressed as[3]

$$p(\vec{r}) = \frac{k\rho c}{(2\pi)^2} \iint_{(\alpha^2+\beta^2)\leq k^2} \frac{A(\alpha,\beta)}{\sqrt{k^2-\alpha^2-\beta^2}} e^{-j(\alpha\xi+\beta\zeta+\gamma\eta)} d\alpha d\beta \qquad (10)$$

where $\gamma = \sqrt{k^2-\alpha^2-\beta^2}$. This equation says that for any (α,β), there exists a plane wave component in this representation, the direction of propagation of this plane wave being given by the cosine directors

$$\left[\frac{\alpha}{k}, \frac{\beta}{k}, \frac{\gamma}{k}\right] \qquad (11)$$

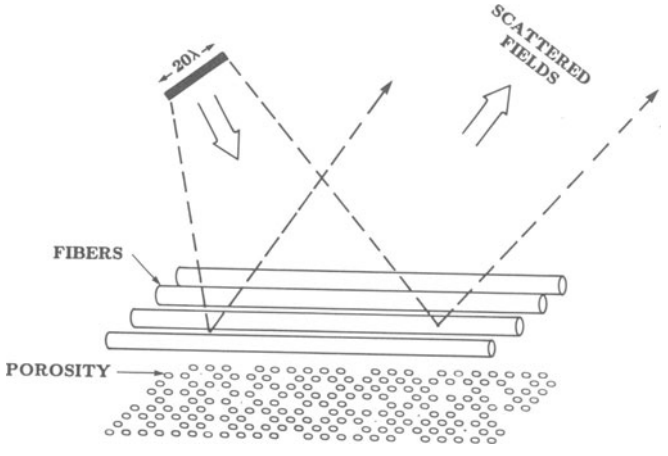

Fig. 10. The radiation problem for determining the directional windows in which the porosity return exceeds the fiber return.

The complex amplitude of each such plane wave is given by

$$\frac{A(\alpha,\beta)}{\sqrt{k^2-\alpha^2-\beta^2}} \tag{12}$$

In the plane wave expansion in (10), we have ignored the evanescent waves, which contribute little beyond 10λ from the transducer. The amplitude function $A(\alpha,\beta)$ in (10) may be obtained by a simple inverse Fourier transformation of the aperture fields in the transducer.

The advantage of this plane wave spectrum representation is that the total scattered field by either the fibers or the voids may now be expressed as a sum of the scattered fields for each plane wave separately. In computing the scattered fields for each plane wave, we assumed that each fiber and each void could be modeled as an inhomogeneity in both density and compressibility, and then we used the Born approximation. In other words, the fibers and the voids were considered to be weakly scattering density and compressibility inhomogeneities. Although this approximation definitely does not apply in composites, we used it to basically prove the concept that randomly located spherical inhomogeneities could be detected and, perhaps their parameters estimated, in the presence of cylindrical and periodic inhomogeneities. (After all, if this concept failed under the vastly simplifying assumption of the Born approximation, there would be no chance of its working in the presence of further complications introduced by the multiple scattering and anisotropies of an actual composite.) Given this justification for the weak scattering assumption, the scattered field caused by a fiber for

each plane wave in the plane wave spectrum representation of Eq. (10) was written as

$$p_s(\vec{r}) = e^{jk_s z}\sum \varepsilon_m j^m \cos(m\phi)[J_m k_r r) + D_m H_m^{(1)}(k_r r)] \tag{13}$$

where

$$D_m = \frac{J_m(k_e a)J'_m(k_r a) - \alpha J'_m(k_e a)J_m(k_r a)}{\alpha J'_m(k_e a)H_m^{(1)}(k_r a) - J_m(k_e a)H_m^{(1)}(k_r a)} \tag{14}$$

J_m and $H_m^{(1)}$ are, respectively, the Bessel functions and cylindrical Hankel functions. Also in these equations, k_r, k_e and α are given by

$$k_r^2 = k^2 - k_z^2$$

$$k_e^2 = \frac{\rho_e \kappa_e}{\rho \kappa} k_r^2 \tag{15}$$

and

$$\alpha^2 = \frac{\kappa_e \rho}{\kappa \rho_e}$$

The parameters ρ and κ are the density and the compressibility, respectively, of the background medium. The parameters ρ_e and κ_e are, respectively, the density and the compressibility within the fiber inhomogeneity. Equation (13) applies when the cylindrical fiber is illuminated with a plane wave whose direction of propagation subtends an arbitrary angle with the axis of the fiber. The cosine of this angle is k_z/k. Appropriate transformations between the direction cosines in (11) and those for the plane wave propagation direction implied in (13) were carried out.

Although the plane wave expansion in (10) applies for the completely general case of radiation into three-dimensional space, its two dimensional analog was actually used in the computer simulations. The two-dimensional case is depicted in Fig. 11. The transducer is a 20λ wide piston radiator and is infinitely long in directions perpendicular to the plane of the paper. This transducer illuminates a coplanar strip of fibers. The density of the fibers was assumed to be 0.4 times the density of the background medium, while their compressibility was assumed to be the same. Below the fibers were placed randomly located voids, their density and compressibility corresponding to those of air.

The solid line in Fig. 12 is a polar plot of the computed scattered fields from the fibers when ϕ in Fig. 11 is made zero, in other words, when the transducer illumination is broadside. In this figure both the radii of the fibers and of the voids are equal to 0.1λ. The dashed line represents the scattered field by the voids. The mean distance between the voids is 0.8λ. The vertical scale in Fig. 12 should be viewed with caution, since the plot is not in the usual rectangular form, but in a polar format. It is clear from

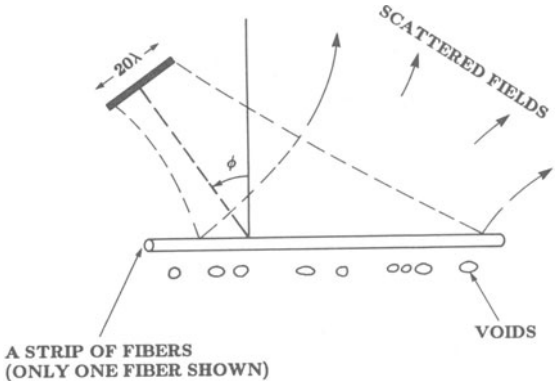

Fig. 11. The two dimensional version of the radiation problem shown in Fig. 10.

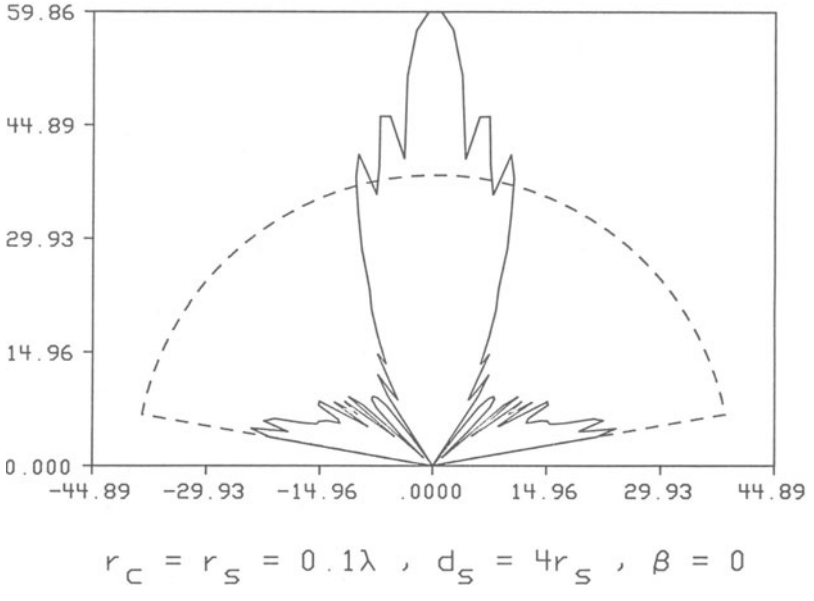

Fig. 12. The solid line shows a computer generated polar plot of the scattered returns from the fibers when the angle ϕ of the illumination in Fig. 11 is zero. The dotted line shows the backscattered return from randomly located voids.

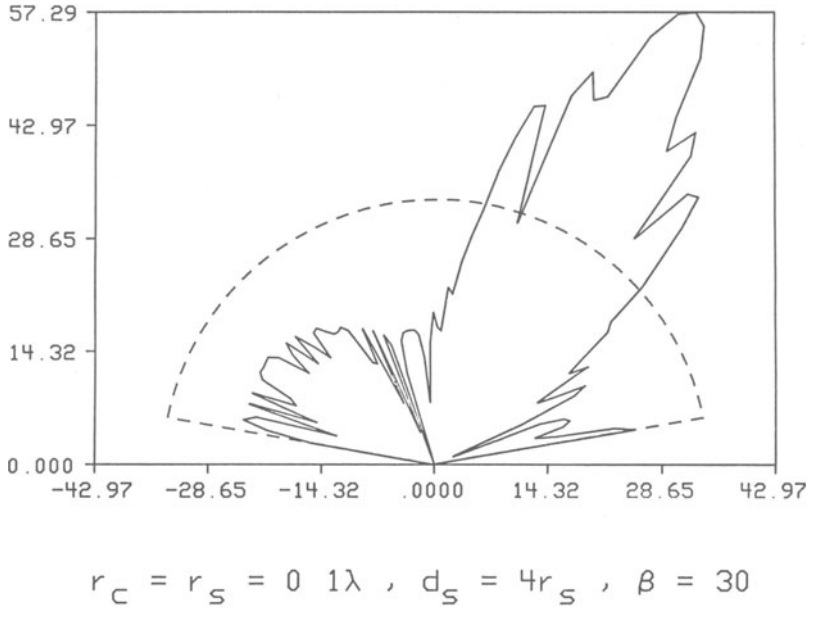

Fig. 13. Same as in Fig. 12 except that the angle of illumination, ϕ, is equal to 30°.

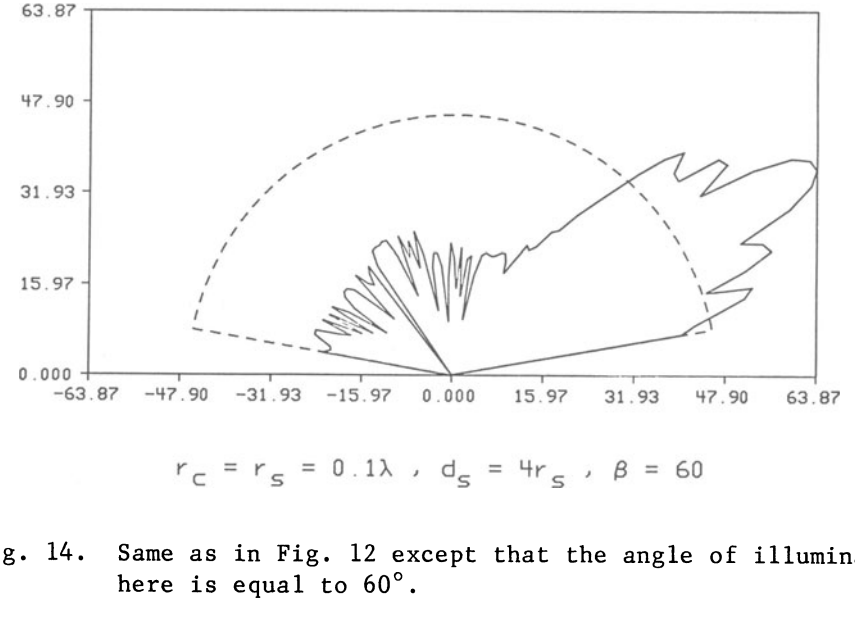

Fig. 14. Same as in Fig. 12 except that the angle of illumination here is equal to 60°.

this figure, that for broadside illumination with a 20λ transducer, the fiber backscatter would overwhelm the porosity backscatter.

When the angle of illumination, ϕ in Fig. 11, is equal to 30°, the computed scattered fields from the fibers are shown by the solid line in Fig. 13 for the case of the mean distance between the voids being equal to 0.4λ. The rest of the parameters are the same as before. One can now see that the backscatter from the porosity toward the illuminating transducer now exceeds the return in the same direction by the fibers.

If the angle ϕ of illumination is increased to 60°, the corresponding results are shown in Fig. 14.

CONCLUSION

We have presented some very preliminary computer simulation results that establish the feasibility of using oblique incidence ultrasound for the detection of porosity. Our results at this time suffer from the limitations imposed by the use of the Born approximation and also by our neglecting multiple scattering and anisotropies inherent to actual composites. In addition to the experimental verification of the results already obtained, we are also hoping to devise heuristic procedures for taking into account these neglected phenomena.

ACKNOWLEDGEMENT

This work was sponsored by the Center for Advanced Nondestructive Evaluation, operated by the Ames Laboratory, USDOE, for the Air Force Wright Aeronautical Laboratories/Materials Laboratory and the Defense Advanced Research Projects Agency under Contract No. W-7405-ENG-82 with Iowa State University.

REFERENCES

1. P.M. Morse and K.U. Ingard, "Theoretical Acoustics," McGraw-Hill, New York.
2. R.L. Crane, private communication. (The idea that the enhancement in the received backscattered signal, when a flat piece of composite is illuminated at oblique angles, be used for porosity detection was first suggested to the authors by Dr. R.L. Crane of Wright-Patterson Air Force Labs.)
3. D. Nahamoo and A.C. Kak, "Ultrasonic Diffraction Imaging," Technical Report TR-EE 82-20, School of Electrical Engineering, Purdue University, August 1982.

DISCUSSION

D.E. Yuhas (Sonoscan): Does this model take multi-ply structures into account?

A.C. Kak (Purdue University): In this comparison simulation, we have only one layer of fibers and one layer of porosity, but once you have a basic program working, it is easy then to introduce fibers going in different directions. We have done that, yes.

D.E. Yuhas: Does that require that you go through the calculation? Do you have to find windows in exactly the right spot?

A.C. Kak: That's true. Now, the window location would be in three dimensions, and so it would take some fancier visualization, I suppose, but I think we have done the most difficult part, and the rest should not be that hard.

J.H. Rose (Ames Laboratory): You are not going to have perfect long-range order in the fiber position. Have you considered the effect of this on the very directional nature of the scattering from the random model?

A.C. Kak: No, I think the directionality would be controlled more by the overall aperture, by the overall size of the illumination. Moreover, they are quite periodic. If you were given a choice between a periodic model and a random model for fibers, I would go toward the periodic side.

J.H. Rose: So you don't think that short-range order would be a better description than long-range order?

A.C. Kak: I believe not.

T.J. De Lacy (Ford Aerospace): That's interesting, but you know, the resin in those epoxy-graphite surfaces transfers load into fibers, and for structural applications, the fibers count and dominate. When you fabricate a composite, you frequently trap voids at the tows, and those tows, of course, are made up of bundles of fibers that have directional features. We developed capability to determine relaxation potential in the material, and we subjected reconditioning based on the amount of resin which is able to take up that local stress between those directional voids, and a directional index is used to grade the relative stability potential in the material. In fact, isolated voids in the composite are not very important. Porosity may not be terribly important but local voids, where they actually interfere with the transfer load to the fiber, become very important.

A.C. Kak: No, I wasn't modeling them in isolated voids. They are quite densely packed, but I was saying there is no order, there is no periodicity to the locations of the voids, and there is no reason to expect periodicities.

T.J. De Lacy: I believe it's the separation between voids that matters. If you are talking about porosity, you may talk about random microporosity, but large voids tend to coalesce and be trapped, and they tend to have directional features, and they're the ones that cause a lot of problems.

A.C. Kak: Yes, but they are also easy to detect once they merge and become delaminations. Then of course, it is not that big a challenge to find them.

T.J. De Lacy: It is a challenge to characterize them, because while you may detect an individual void, it is very important that you determine how that plane interrelates to the features of the construction of the composite.

A.C. Kak: Yes, according to the chart we were given, my understanding was that the idea was to characterize this microporosity before it became a large delamination, and that's what we have been perusing. My assumption is consistent with that.